VASCULAR BIOLOGY

# Angiophagy Prevents Early Embolus Washout But Recanalizes Microvessels Through Embolus Extravasation

Jaime Grutzendler,[1,2]* Sasidhar Murikinati,[1] Bennett Hiner,[3†] Lingling Ji,[1] Carson K. Lam,[3] Taehwan Yoo,[3] Shobhana Gupta,[1] Brian P. Hafler,[4] Ron A. Adelman,[4] Peng Yuan,[1] Guadalupe Rodriguez[1,3]

**Occlusion of the microvasculature by blood clots, atheromatous fragments, or circulating debris is a frequent phenomenon in most human organs. Emboli are cleared from the microvasculature by hemodynamic pressure and the fibrinolytic system. An alternative mechanism of clearance is angiophagy, in which emboli are engulfed by the endothelium and translocate through the microvascular wall. We report that endothelial lamellipodia surround emboli within hours of occlusion, markedly reducing hemodynamic washout and tissue plasminogen activator–mediated fibrinolysis in mice. Over the next few days, emboli are completely engulfed by the endothelium and extravasated into the perivascular space, leading to vessel recanalization and blood flow reestablishment. We find that this mechanism is not limited to the brain, as previously thought, but also occurs in the heart, retina, kidney, and lung. In the lung, emboli cross into the alveolar space where they are degraded by macrophages, whereas in the kidney, they enter the renal tubules, constituting potential routes for permanent removal of circulating debris. Retina photography and angiography in patients with embolic occlusions provide indirect evidence suggesting that angiophagy may also occur in humans. Thus, angiophagy appears to be a ubiquitous mechanism that could be a therapeutic target with broad implications in vascular occlusive disorders. Given its biphasic nature—initially causing embolus retention, and subsequently driving embolus extravasation—it is likely that different therapeutic strategies will be required during these distinct post-occlusion time windows.**

## INTRODUCTION

Thromboembolic occlusions of the microvasculature play a critical role in the pathogenesis of conditions such as stroke (*1*), myocardial infarction (*2*, *3*), pulmonary embolism (*4*), retinal ischemia (*5*), and others (*6*). Occlusions occur as a result of spontaneous clot formation, dislodgment of microemboli from atherosclerotic plaques, or after cardiovascular surgical interventions (*7*). Furthermore, administration of thrombolytic agents to break down large clots can generate embolic fragments that occlude downstream microvessels (*2*). Despite their small size, microemboli can cause significant tissue ischemia and morbidity (*8*, *9*), and their cumulative effect over time can lead to cognitive impairment (*9*, *10*), decreased myocardial contractility, and renal dysfunction (*11*, *12*).

The fibrinolytic system and hemodynamic forces clear a large portion of acute thromboemboli; however, it is not clear how effectively they are able to eliminate blood clots in the microvasculature (*13*). Furthermore, fibrinolytic enzymes cannot remove occluding materials composed of cholesterol crystals, calcified emboli, and cellular debris, which are not susceptible to fibrinolysis. We have recently discovered a novel mechanism by which vessels are recanalized in the brain microcirculation. After embolic occlusion with diverse materials such as fibrin, blood clots, or cholesterol crystals, the endothelium adjacent to the occlusion site completely engulfs the emboli. This engulfment is followed by opening of the endothelial barrier and extrusion of the embolus into the surrounding parenchyma, leading to vessel recanalization and flow reestablishment. This process, which we termed angiophagy, occurs between 1 and 6 days after occlusion in mice (*14*, *15*).

Here, we used high-resolution two-photon in vivo imaging and confocal and electron microscopy of mouse brain, lung, kidney, heart, and retina to characterize the time course and cellular features of microvascular embolic washout, fibrinolysis, and angiophagy. We also examined longitudinal retina photographs of patients with embolic events to determine whether angiophagy occurs in humans. We identified several important and previously unknown features of microvascular occlusions and the recanalization process. First, angiophagy is not unique to the brain but, rather, occurs in all organs we tested, suggesting that it is a ubiquitous mechanism of recanalization. Second, we found indirect evidence that transvascular embolus extrusion and vessel recanalization occur in humans. Finally, we show that endothelial engulfment begins as early as 1 hour after embolization in mice and can initially lead to physical retention of emboli within the microvasculature, blocking hemodynamic clearance and disrupting efficient clot fibrinolysis.

The biphasic nature of angiophagy suggests that it is likely to be detrimental during early stages of engulfment, but beneficial for subsequent extravasation and recanalization. Therapeutic targeting of these distinct stages of angiophagy could be relevant for treating a variety of thromboembolic disorders in humans.

## RESULTS

### Microvascular emboli washout by hemodynamic forces and by the fibrinolytic system is inefficient

A mouse model of embolic occlusion was used to investigate the effectiveness of the fibrinolytic system and of hemodynamic forces in inducing emboli degradation and washout. We injected fluorescently labeled fibrin clots either into the internal carotid artery to embolize the brain or retrograde into the left common carotid artery to embolize the heart. Experiments were performed using transgenic mice with endothelial cell–specific fluorescence (*Tie2-GFP*). We tracked the outcome

[1]Department of Neurology, Yale University School of Medicine, New Haven, CT 06510, USA. [2]Department of Neurobiology, Yale University School of Medicine, New Haven, CT 06510, USA. [3]Department of Neurology, Northwestern University Feinberg School of Medicine, Chicago, IL 60611, USA. [4]Department of Ophthalmology, Yale University School of Medicine, New Haven, CT 06510, USA.
*Corresponding author. E-mail: jaime.grutzendler@yale.edu
†Deceased.

of individual microvascular occlusions either by time-lapse transcranial in vivo two-photon imaging of meningeal microvessels or by confocal microscopy of brain and heart sections. We observed clot degradation and washout in the first 6 hours after embolization (Fig. 1A); however, the rate of emboli washout declined steadily in both the brain and the heart (Fig. 1, B and C). After the initial 6 hours, there was minimal additional washout, leaving a substantial microvascular embolic burden.

The relatively high washout failure was not due to a lack of initial accessibility of fibrinolytic proteins, such as tissue plasminogen activator (tPA), as evidenced by the preservation of some plasma flow in the occluded microvascular segment (Fig. 1D) and staining for tPA (Fig. 1E). tPA labeling declined over time, with little residual labeling after 6 hours (Fig. 1, E and F), coinciding with the decline in emboli washout (Fig. 1B). Intravenous administration of recombinant tPA modestly im-

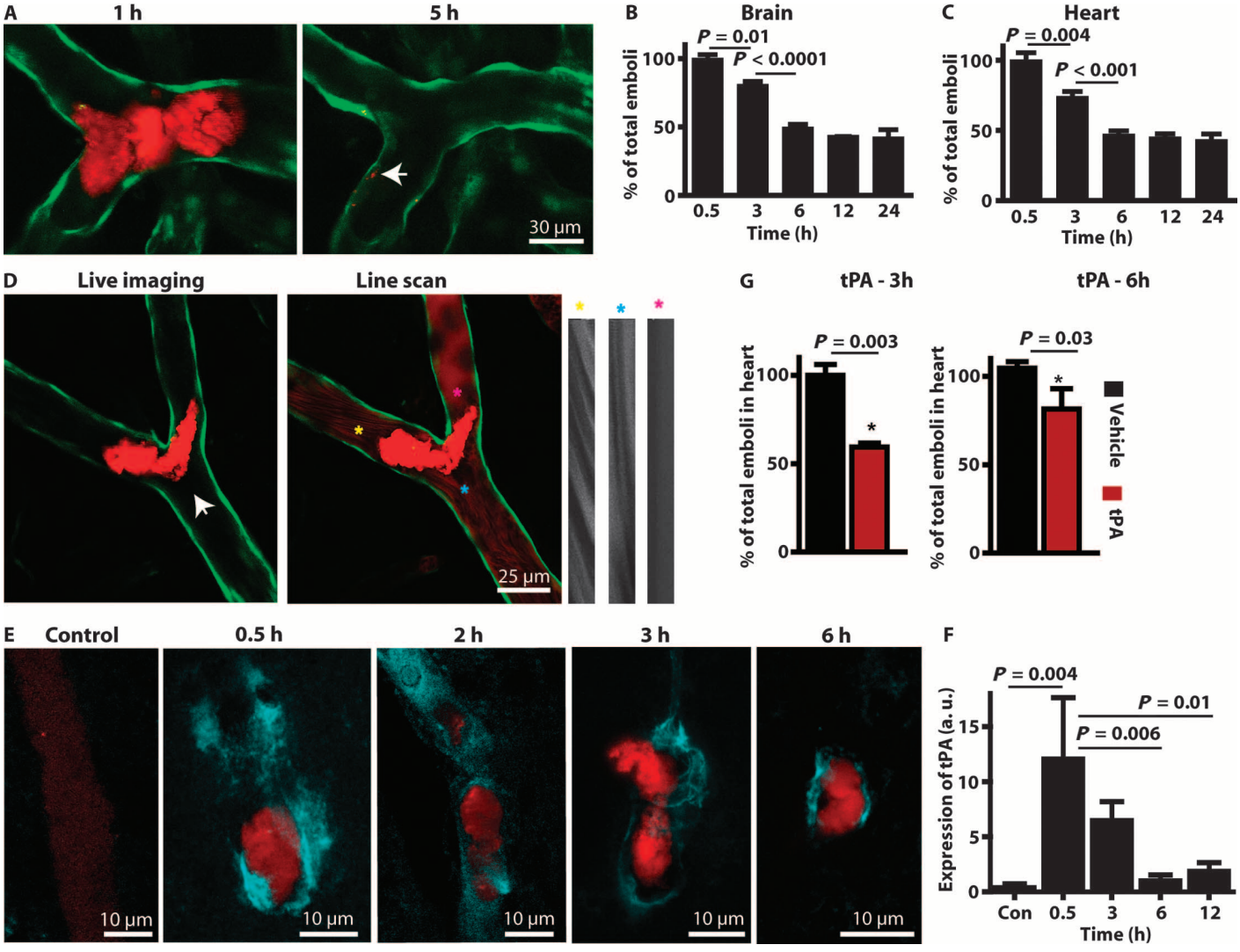


**Fig. 1. Microvascular emboli washout has a substantial failure rate.** (**A**) Two-photon in vivo imaging of meningeal vessels 1 and 5 hours after embolization with fluorescent fibrin clots (red). A residual clot fragment near the green fluorescent protein (GFP)–labeled endothelium at 5 hours is indicated by a white arrow. (**B**) Number of clots remaining in brain microvessels over time after embolization expressed as a percentage of clots found at the first time point ($n$ = 3 mice per time point and 4654 total emboli). (**C**) Number of clots remaining in cardiac microvessels over time after embolization expressed as a percentage of clots found at the first time point ($n$ = 3 mice per time point and 6984 total emboli). (**D**) In vivo two-photon imaging of a fibrin embolus (red) lodged in a leptomeningeal microvessel 4 hours after embolization. White arrow indicates direction of blood flow. Two-photon line scan images (in gray scale bars) after fluorescent dextran (red) administration show plasma and some residual blood flow within vessels downstream (yellow and pink asterisks) and upstream (blue asterisk) of occluding embolus. (**E**) Immunohistochemical labeling of endogenous tPA in unoccluded control brain microvessels and in occluded microvessels over time after embolization. (**F**) tPA fluorescence intensity around fibrin clots in cerebral microvessels at various time points after embolization ($n$ = 3 mice per time point and 73 total occlusion events). (**G**) Number of clots (10 to 20 μm) that remained in cardiac microvessels 12 hours after embolization in mice treated with intravenous saline (black bar) or recombinant tPA (red bar) at 3 hours ($n$ = 3 mice per time point and 1613 total emboli) or 6 hours ($n$ = 3 mice per group and 1882 total emboli) after embolization. Data reported as a percentage of clots found at the first time point. $P$ values in (B), (C), and (F) were determined by one-way analysis of variance (ANOVA) with Tukey's multiple comparison test. $P$ values in (G) were determined by unpaired $t$ test. All data are means ± SEM.

proved the overall clot washout, with the greatest effect observed when tPA was administered within 3 versus 6 hours of embolization (Fig. 1G). The gradual reduction in tPA coupled with the overall lack of hemodynamic flow could partly explain the low efficiency of embolic washout in microvessels.

### Endothelial lamellipodia engulf emboli and prevent their early washout

We imaged *Tie2-GFP* mice at various time points after embolization to characterize the early stages of endothelial remodeling after occlusion. In both the brain and the heart, as early as 3 hours after embolization,

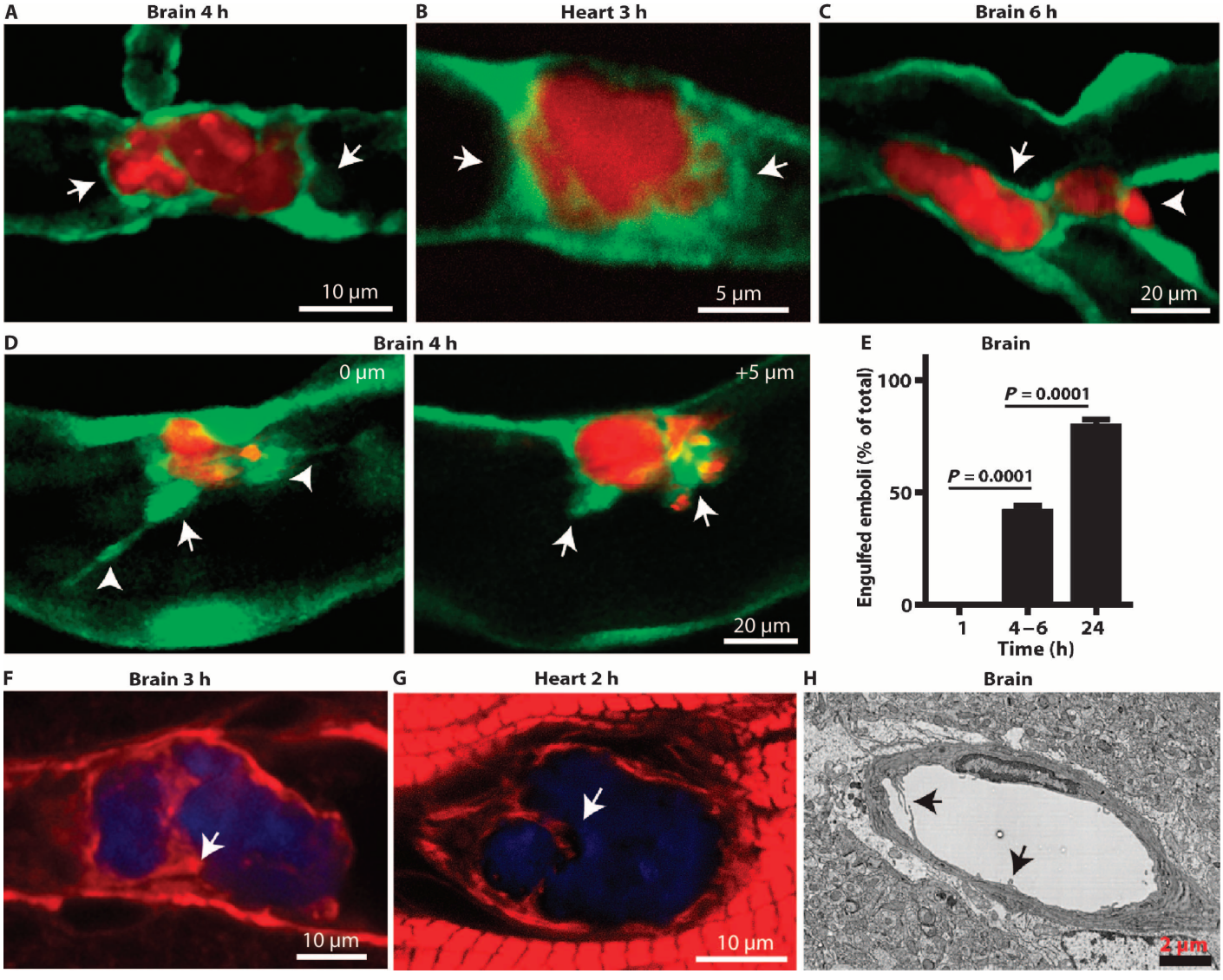


**Fig. 2. Endothelial lamellipodia engulf and retain emboli within microvessels.** Images of fibrin clots within vessels taken from *Tie2-GFP* mice. (**A**) In vivo image 4 hours after embolization shows fibrin clot (red) blocking the vessel lumen and projections from the adjacent endothelium (arrows) contacting the clot surface. (**B**) Confocal image of a heart microvessel 3 hours after embolization shows an occluding fibrin embolus (red) that is completely enveloped by endothelial lamellipodia (arrows). (**C**) In vivo image of a brain microvessel shows a fibrin embolus completely enveloped by endothelial lamellipodia (arrows) 6 hours after embolization. The tip of the embolus is in the process of being extruded out of the endothelial wall (arrowhead). (**D**) Two-photon in vivo imaging of a leptomeningeal arteriole (green) at 4 hours after embolization shows two optical sections of a clot at different *z* positions. At $z = 0$ μm, endothelial processes (arrowheads) with bulbous ends (arrow) emanate from opposing sides of the vessel toward the clot. At $z = +5$ μm, the clot appears to be partially engulfed and retained in the vessel by these processes (arrows). (**E**) Percentage of emboli in microvessels that were engulfed by endothelial lamellipodia at various time points in *Tie2-GFP* mice (means ± SEM; $n = 52$ mice and 309 total emboli). *P* values were determined by one-way ANOVA with Tukey's multiple comparison test. (**F**) Confocal image of an intraparenchymal cerebral microvessel labeled with phalloidin (red) shows the endothelial projections (arrow) surrounding a fibrin clot (blue) (see movie S1 for Z-stacks). (**G**) Confocal image 2 hours after embolization of a cardiac microvessel occluded by a fibrin clot (blue), and is labeled with phalloidin (red). Multiple phalloidin-positive filopodia project toward the embolus (arrow) (see movie S2 for Z-stacks). (**H**) TEM image from the adult mouse cortex shows long endothelial filopodia (black arrows) present in an unoccluded microvessel (see movies S3 and S4 for Z-stacks).

distinct lamellipodia projected toward the embolus from adjacent endothelial cells (Fig. 2, A to D). Within 4 to 6 hours of embolization, more than 40% of emboli were almost completely enveloped by these projections (Fig. 2E). These lamellipodia had strong F-actin labeling [Fig. 2, F and G, and movies S1 (brain) and S2 (heart)], suggesting active cytoskeletal remodeling. Transmission electron microscopy (TEM) demonstrated that, even in the absence of any embolization, endothelial cells in brain microvasculature had multiple filopodial protrusions (2 to 10 per individual TEM section) (Fig. 2H and movies S3 and S4). This raises the possibility that the larger protrusions observed after embolization are extensions of these preexisting filopodia.

In capillaries, clots generally blocked blood flow completely and were robustly enveloped by the adjacent endothelium (Fig. 2, A and B). In larger arterioles (>20 μm in diameter), we observed partially occluding clots attached to the vessel wall, which appeared to be held in place by the endothelial processes, even against the hemodynamic forces (Fig. 2, C and D). This suggests that endothelial lamellipodia engulfing the emboli are capable of physically preventing their hemodynamic washout. Furthermore, given the temporal coincidence between the lamellipodial engulfment (Fig. 2E) and the decline in tPA immunolabeling (Fig. 1, E and F), it is also possible that endothelial engulfment limits the access of plasma and tPA to the emboli, further reducing the effectiveness of fibrinolysis and washout.

### Capillaries and arterioles can be recanalized by angiophagy, leading to long-term vascular sparing

Brain parenchymal microvessels ranging from 8 to 15 μm, when occluded with emboli for greater than 24 hours, begin a cellular process to extrude the emboli through the endothelial barrier, resulting in vessel recanalization (*14*). We sought to determine the maximal embolus size that could be successfully extruded out of cerebral vessels. Given that most large arterioles in the mouse brain are extraparenchymal, we focused on leptomeningeal vessels, which are easily accessible for transcranial in vivo two-photon imaging (*16*). We examined vascular dynamics in *Tie2-GFP* mice embolized with fluorescently labeled fibrin clots or cholesterol emboli ranging

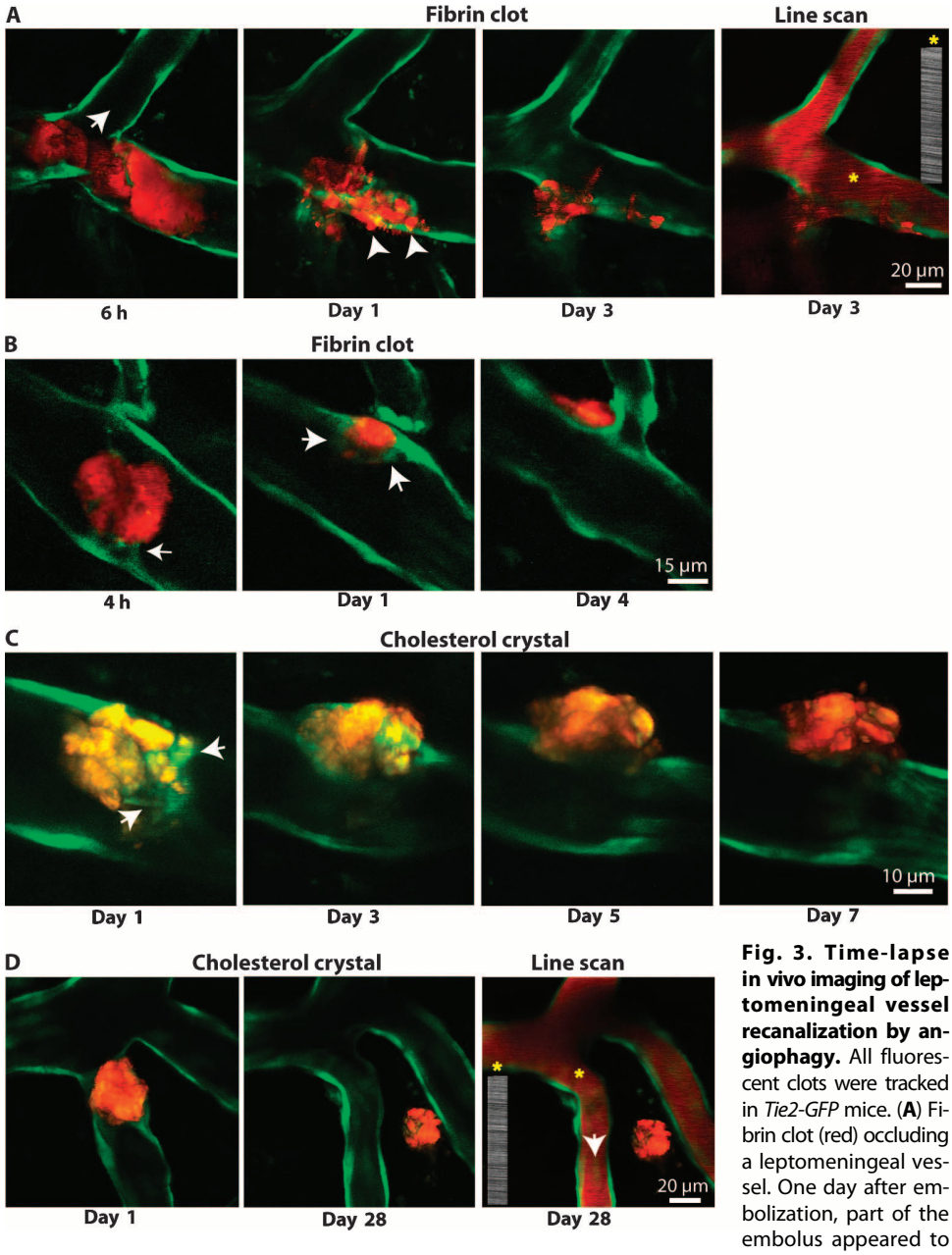


**Fig. 3. Time-lapse in vivo imaging of leptomeningeal vessel recanalization by angiophagy.** All fluorescent clots were tracked in *Tie2-GFP* mice. (**A**) Fibrin clot (red) occluding a leptomeningeal vessel. One day after embolization, part of the embolus appeared to have been washed out. The remaining embolus was engulfed by the endothelium (in green) and broken down into several small pieces (arrowheads). Three days after embolization, the disintegrated emboli fragments were mostly extravasated out of the lumen. Vessel recanalization and restoration of blood flow were demonstrated using intravenous red fluorescent dextran injection and subsequent line scan imaging (yellow asterisk). (**B**) Fibrin embolus (red) appeared to be retained within the microvessel by fine endothelial lamellipodia by 4 hours after embolization. By day 1, the same clot has been partly washed out, and the remaining fragment was engulfed and extravasated by day 4. (**C**) Cholesterol crystals in cerebral microvessels. At day 1 after embolization, processes projecting from the endothelium (arrows) surrounded the crystal. By day 3, the occluding embolus was completely engulfed by an envelope formed by the endothelium. By day 5, the embolus was partially extravasated from the vessel lumen. The cholesterol crystal was cleared from the lumen and extruded completely into the perivascular space by day 7. (**D**) Live imaging 1 day after embolization with cholesterol crystals demonstrates an occluding embolus blocking blood flow in a cerebral microvessel. Twenty-eight days after embolization, the cholesterol crystal remained in the perivascular space. Two-photon line scan imaging of blood flow was performed after red fluorescent dextran intravenous injection before imaging. The line scan image shown in gray scale demonstrates blood flow and lumen patency at the site of previous embolization (arrow).

from 20 to 50 μm. As observed in the smaller parenchymal microvessels (*14*), clot extravasation and recanalization of larger meningeal arterioles occurred within 1 to 6 days (10 of 11 fibrin clots imaged in vivo had extravasated by day 4) (Fig. 3, A and B). Cholesterol crystals were extravasated more slowly, with complete vessel patency generally restored within 3 to 8 days after occlusion (Fig. 3C). The faster rate of extravasation of fibrin clots may be, in part, due to their frequent lysis into smaller fragments, which may facilitate endothelial engulfment (Fig. 3, A and B). Thus, fibrinolysis may contribute to more efficient angiophagy-mediated vessel recanalization.

Given the variability in the timing of angiophagy, it is likely that many vessels are exposed to hypoxia for significant periods of time before they are recanalized. Nevertheless, vessels demonstrated normal morphological appearance and continuous blood flow 1 month after recanalization (7 of 7 vessels that underwent angiophagy had continuous blood flow) (Fig. 3D), and their ultrastructure appeared normal

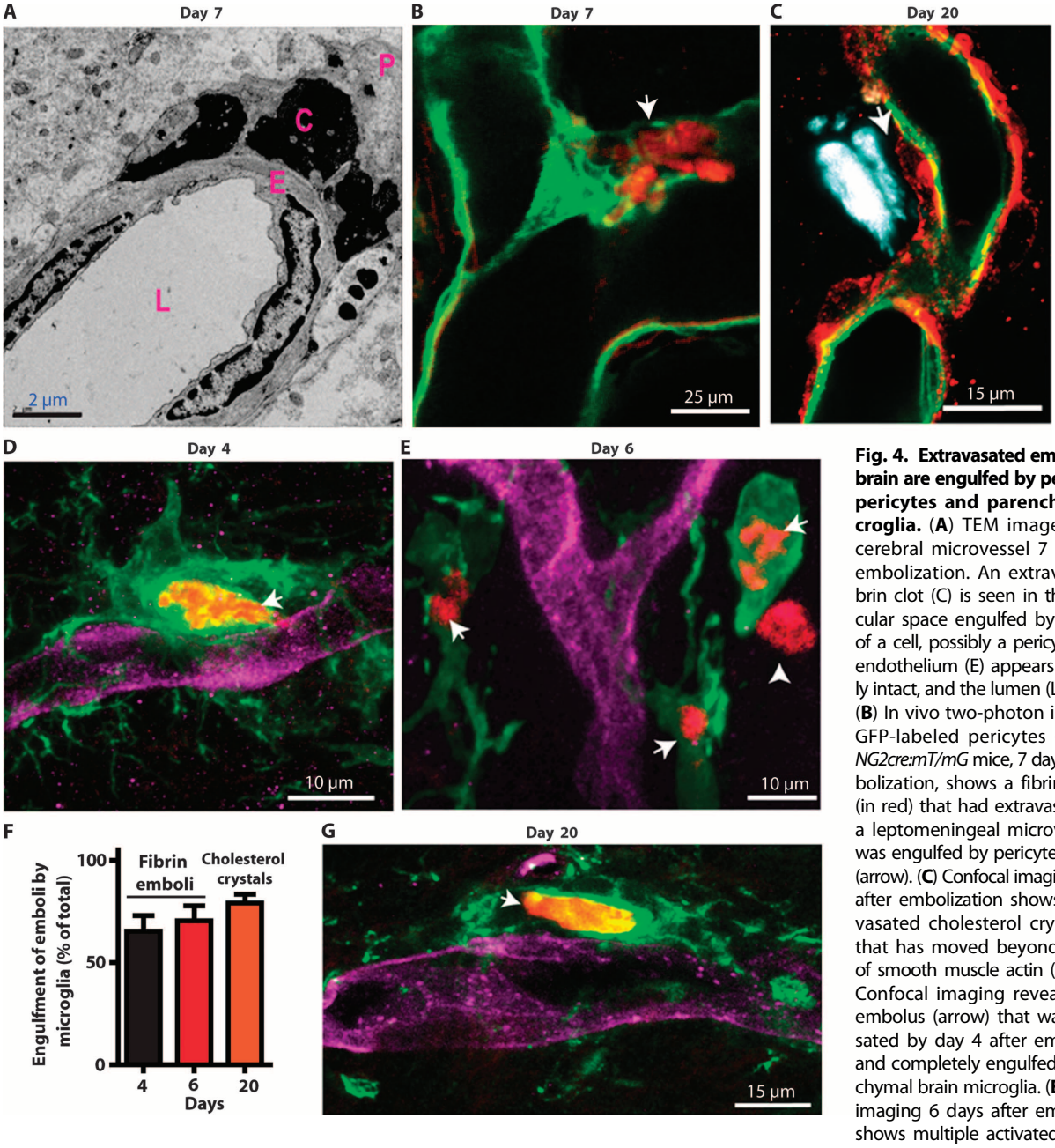


**Fig. 4. Extravasated emboli in the brain are engulfed by perivascular pericytes and parenchymal microglia.** (**A**) TEM image shows a cerebral microvessel 7 days after embolization. An extravasated fibrin clot (C) is seen in the perivascular space engulfed by processes of a cell, possibly a pericyte (P). The endothelium (E) appears structurally intact, and the lumen (L) is patent. (**B**) In vivo two-photon imaging of GFP-labeled pericytes (green) in *NG2cre:mT/mG* mice, 7 days after embolization, shows a fibrin embolus (in red) that had extravasated from a leptomeningeal microvessel and was engulfed by pericyte processes (arrow). (**C**) Confocal imaging 20 days after embolization shows an extravasated cholesterol crystal (blue) that has moved beyond the layer of smooth muscle actin (in red). (**D**) Confocal imaging reveals a fibrin embolus (arrow) that was extravasated by day 4 after embolization and completely engulfed by parenchymal brain microglia. (**E**) Confocal imaging 6 days after embolization shows multiple activated microglia engulfing embolic fragments (arrows) and a large fragment that has not yet been engulfed (arrowhead). (**F**) Percentage of extravasated emboli engulfed by parenchymal microglia at different time points after embolization. Quantifications at days 4 and 6 were done in mice embolized with fibrin emboli, whereas quantifications at day 20 were with cholesterol crystals owing to the difficulty in visualizing degraded fibrin clots. Data are means ± SEM ($n$ = 3 mice per time point and 61 total extravasated events). (**G**) Confocal imaging in the brain shows a cholesterol crystal (arrow) that has extravasated 20 days after embolization, and is engulfed by activated microglia (in green).

by TEM (Fig. 4A). Thus, once recanalized, previously occluded vessels appear to be permanently spared.

### Extravasated emboli are gradually degraded by pericytes and microglia

TEM revealed that fragments of extravasated fibrin emboli appeared to be surrounded by processes from adjacent perivascular cells (Fig. 4A). To further characterize this phenomenon, we analyzed angiophagy in transgenic mice with fluorescent pericytes (*NG2cre:mT/mG*) using in vivo two-photon imaging. Soon after extrusion from the vessel lumen, fibrin emboli were engulfed by pericytes where they resided for several days (Fig. 4B). Emboli were eventually transported into the brain parenchyma, as evidenced by their location beyond the labeled smooth muscle actin (Fig. 4C), and their engulfment and degradation by parenchymal microglia (Fig. 4, D and E, and fig. S1). Most of the extravasated cholesterol emboli were also engulfed by microglia (Fig. 4F), but in contrast to fibrin emboli, they underwent almost no degradation and remained in the juxtavascular brain parenchyma for many months (Figs. 3D and 4G).

### Angiophagy is a mechanism of recanalization in the heart microvasculature

Similar to the brain, microvessels in the heart and other organs are susceptible to occlusion by emboli generated from rupture of atherosclerotic plaques and thrombi (*17*) or from surgical cardiovascular interventions (*11*, *18*). We sought to determine whether recanalization by angiophagy is a specialized feature of the cerebral microvasculature or whether it is also present in vessels outside the brain. We embolized various organs in mice with fluorescently labeled fibrin or cholesterol emboli. Owing to limitations of organ accessibility, we did not image microvessels in vivo outside of the brain. High-resolution confocal microscopy in fixed tissues revealed that the endothelium adjacent to emboli in various vascular beds, for example, in cardiac microvessels, underwent an identical multistep process of engulfment and embolus extravasation as the one observed in the brain in vivo (Fig. 5, A to E). Within the first 3 days after occlusion, emboli were generally found to be enveloped by projections from the adjacent endothelium (Fig. 5A). Concurrently, a breach formed in the abluminal vessel wall (Fig. 5, A, B, D, and E), through which the emboli were progressively shifted out of the vessel and a lumen was reestablished (Fig. 5, B to E). The time course of embolus extravasation in the heart was similar to that in the brain (*14*), and by 4 days after embolization, more than 70% of the fibrin clots had undergone extravasation (Fig. 5F).

### Angiophagy in lung and kidney has unique cellular features

We next explored the possibility of angiophagy as a mechanism for vessel recanalization in the lung and kidney. We injected emboli into the tail vein and examined the pulmonary vasculature using high-resolution confocal microscopy. Emboli were initially seen occluding the pulmonary microvasculature (Fig. 6A and fig. S2), but subsequently, they were not only transported across the endothelium, like in the brain, but also frequently crossed into the alveolar space (Fig. 6, B to D).

In contrast to the brain and the heart, the extravasation process in the lung was delayed, and even by day 6 after embolization, most

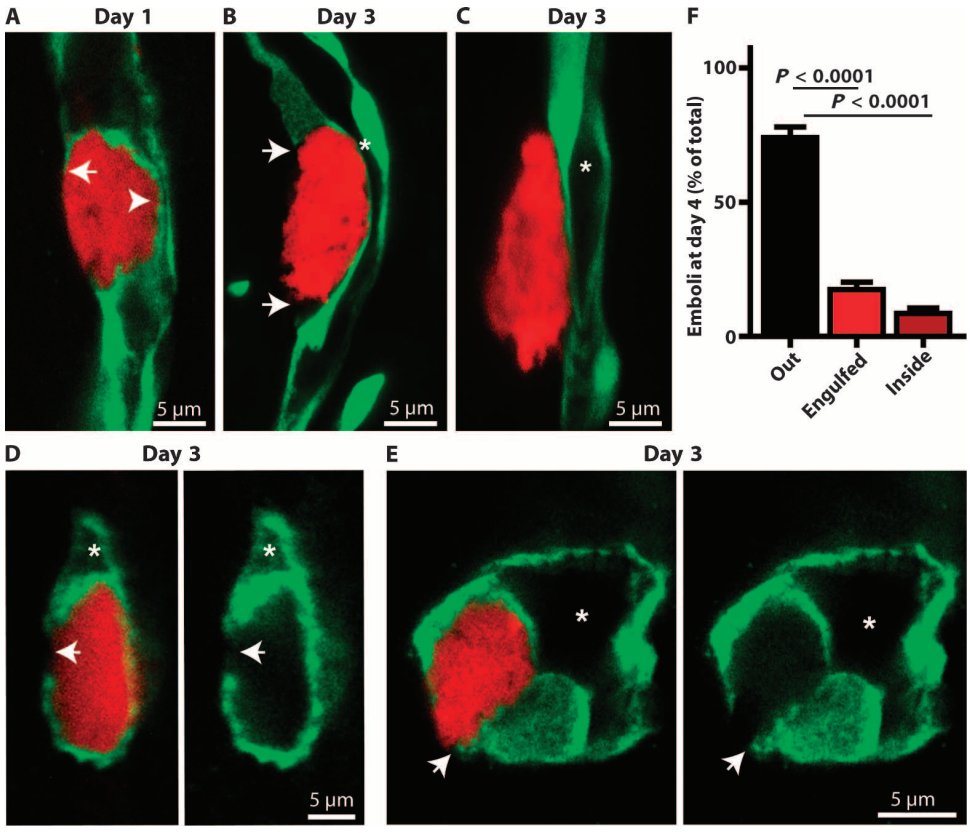


**Fig. 5. Angiophagy leads to vessel recanalization in the cardiac microvasculature.** Confocal imaging of heart tissue from *Tie2-GFP* mice at various time points after embolization with 10 to 20 μm of fibrin emboli (red) demonstrates angiophagy in the coronary microcirculation. (**A**) A fibrin clot is shown 1 day after embolization. The clot is enveloped by lamellipodia from the adjacent endothelium (in green, arrowhead). The original endothelial wall has partially retracted (arrow) forming an opening toward the juxtavascular space. (**B**) A fibrin clot is shown at day 3 after embolization. The abluminal wall has completely retracted (white arrows), and a patent vessel lumen has formed (white asterisk). (**C**) A fibrin clot (red) has completely crossed the endothelial barrier (green), and an apparently patent vessel lumen is observed (white asterisk). (**D**) Transverse views of a microvessel 3 days after embolization of the cardiac microcirculation. Abluminal wall retraction adjacent to the enveloped emboli (white arrow) and a narrow vessel lumen (asterisk) are observed. (**E**) Transverse view of a cardiac microvessel at day 4 after embolization shows the extravasating embolus partially covered by endothelium, after vessel recanalization and lumen recanalization have occurred, and a patent lumen has formed (white asterisk). (**F**) Angiophagy in cardiac microvasculature was quantified as percentage of the total clots that had extravasated 4 days after embolization (means ± SEM; $n = 3$ mice and 60 total emboli). *P* values were determined by one-way ANOVA with Tukey's multiple comparison test.

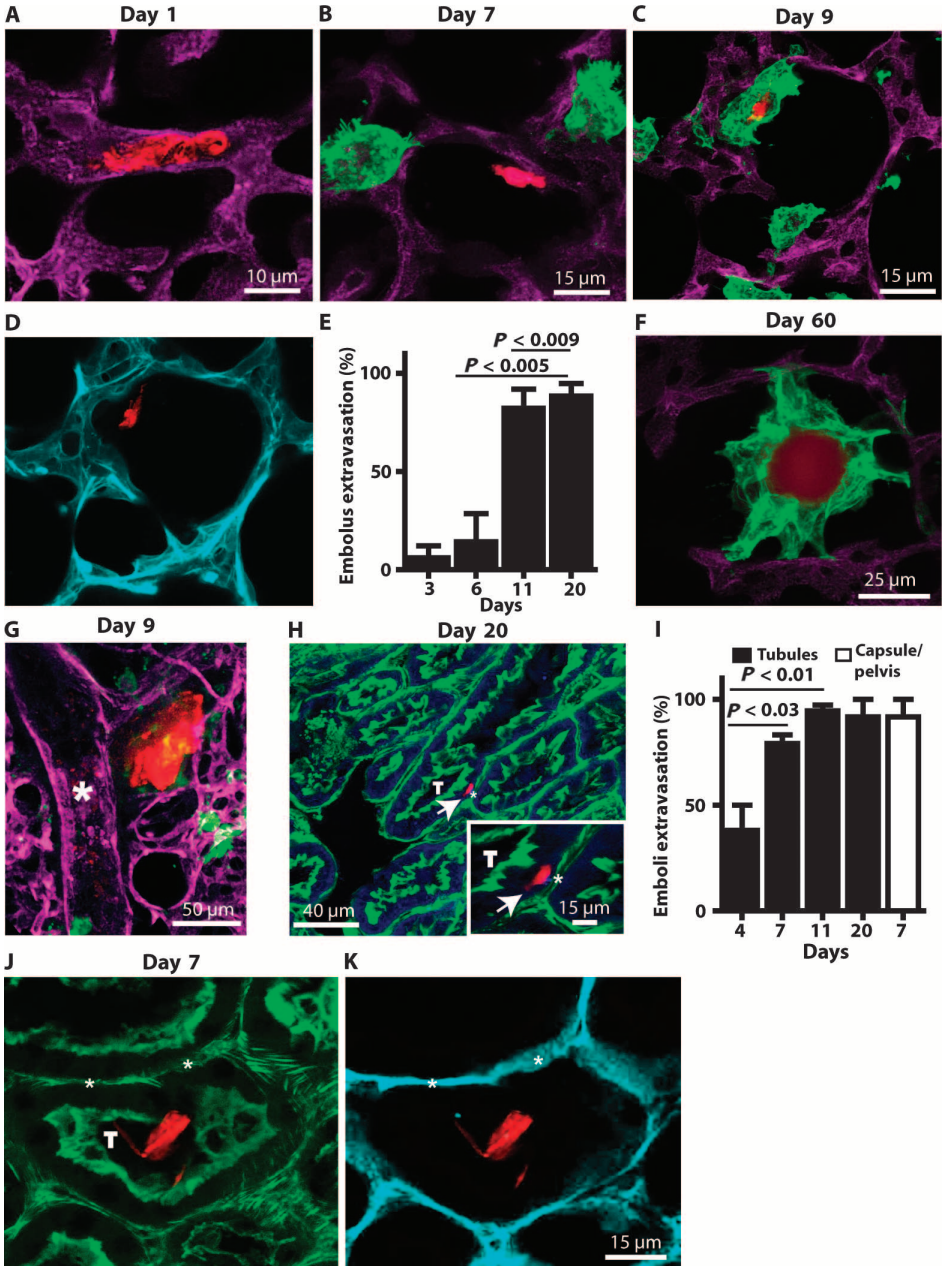


**Fig. 6. Emboli extravasation in pulmonary and renal microcirculation.** (**A** to **D**) Pulmonary fibrin clots (in red) were extravasated from the microvessels (CD31 labeling, in magenta) over time, as seen by confocal imaging. By days 7 and 9, alveolar macrophages (in green, IB4-labeled) were recruited (B) and engulfed a clot (C). (D) Pulmonary vessels near an extravasated clot (red) appear patent (intravascular dye, cyan). (**E**) The number of emboli extravasated was calculated as percent of total emboli imaged at day 0. Data are means ± SEM ($n = 3$ mice per time point and 199 total occlusion events). *P* values were determined by one-way ANOVA with Tukey's multiple comparison test. (**F**) A polystyrene microsphere was extravasated and moved into the alveolar space where it was engulfed by macrophages (green). The macrophages maintained attachments to the alveolar walls via pseudopod-like structures. (**G**) A large (~50 μm) embolus (red) had extravasated outside the vessel (white asterisk) into the alveolar space, 9 days after embolization. (**H**) A fibrin clot (red) extravasated from a peritubular microvessel (asterisk) and embedded in the tubular epithelium (blue autofluorescence), close to the tubular lumen (T), 20 days after embolization. (**I**) Percentage of fibrin clots that had extravasated from microvessels near renal tubules (black bars) at various time points after embolization, and percentage of fibrin clots that had extravasated by 7 days after embolization from microvessels in the renal capsule and pelvis (white bar). Data are means ± SEM ($n = 3$ mice per time point and 100 total occlusion events). *P* values were determined by one-way ANOVA with Tukey's multiple comparison test. (**J** and **K**) Seven days after embolization, a fibrin clot was extravasated from a renal microvessel and appears to be in the process of crossing into the tubular lumen (T) from the adjacent epithelium (F-actin labeled with phalloidin green) (J). The vessels around the embolus are patent by day 7, as evidenced by the intravascular dye (cyan, K).

emboli were still within the microvasculature (Fig. 6E). Nevertheless, the process accelerated after day 6, and by day 11, more than 80% of the occluding emboli had been extravasated (Fig. 6E), and adjacent microvessels appeared to be patent (Fig. 6D). Even polystyrene microspheres (Fig. 6F and fig. S3) and larger fibrin emboli 25 to 100 μm in diameter (Fig. 6G and movie S5) were extravasated and crossed into the alveolar space. Once extravasated into the alveolus, emboli attracted macrophages (Fig. 6B), which phagocytosed (Fig. 6C) and degraded them over time (fig. S2). These alveolar macrophages were labeled with isolectin B4 (IB4) (Fig. 6, B, C, and F, and fig. S2) but rarely expressed the chemokine receptor CX3CR1, suggesting that they were resident alveolar macrophages and not CX3CR1-expressing intravascular macrophages or monocytes (Fig. 7) that had extravasated.

The kidney is also susceptible to occlusions of the microvasculature, which can result in irreversible damage to nephrons and renal failure (*12*, *19*). We found that microvessels in the mouse kidneys removed vascular obstructions similar to the lungs (Fig. 6, H to K, and fig. S4). Extravasation in the renal microvasculature (Fig. 6I) occurred at a rate comparable to those in the brain (*14*) and the heart (Fig. 5D). Similar to the lung, where emboli were cleared by alveolar macrophages (Fig. 6C and fig. S2), emboli in renal microvessels also appeared to have a conduit for permanent removal from the body after extravasation by entering the renal tubules (Fig. 6, H, J, and K), where they could potentially be excreted.

We then explored reasons for the slower rates of angiophagy in the lung. The interactions between CX3CR1-positive macrophages and

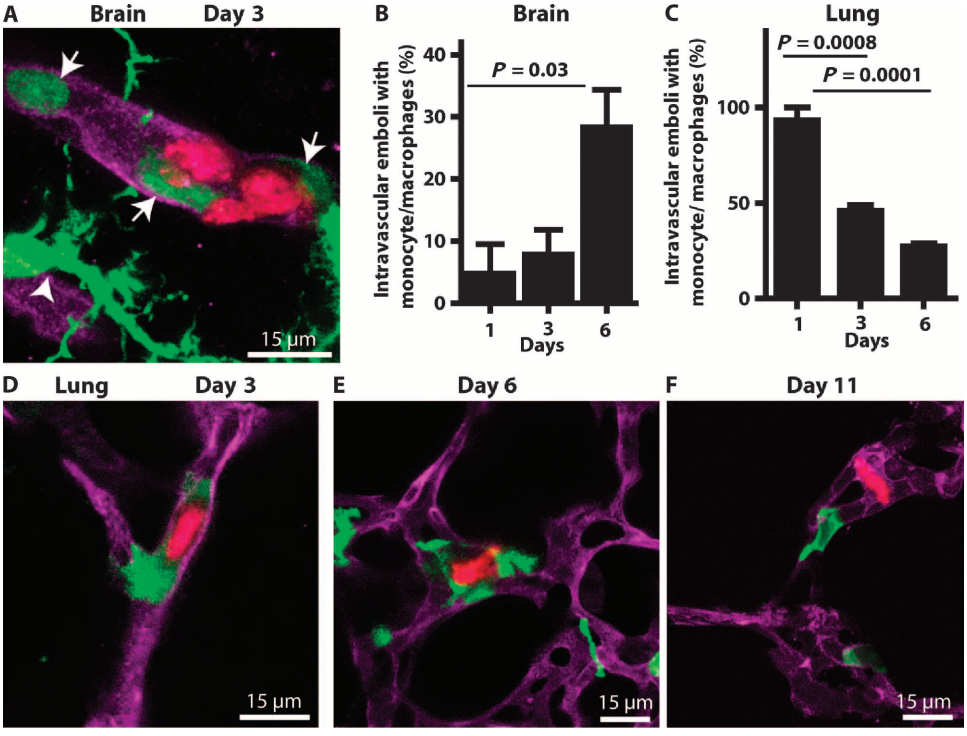


**Fig. 7. Recruitment of monocytes and macrophages to intravascular emboli.** (**A**) Confocal imaging of a fibrin clot (red)–occluded cerebral microvessel [labeled with platelet endothelial cell adhesion molecule (PECAM), magenta] 3 days after embolization. CX3CR1-positive intravascular monocytes (arrows) surrounded the embolus but did not engulf it. CX3CR1-positive parenchymal microglia adjacent to the clot-occluded vessel (arrowhead) had ramified, nonactivated morphologies. (**B**) Percentage of occluding emboli in cerebral microvessels that were surrounded by CX3CR1-positive intravascular monocytes/macrophages at various time points after embolization ($n$ = 3 mice per time point and 53 total occlusion events). (**C**) Percentage of occluding emboli in pulmonary vessels that were surrounded by CX3CR1-positive intravascular monocytes/macrophages at various time points after embolization ($n$ = 3 mice and 74 emboli per time point). Data in (B) and (C) are means ± SEM. $P$ values were determined by one-way ANOVA with Tukey's multiple comparison test. (**D** and **E**) Confocal imaging of pulmonary microvessels at days 3 (D) and 6 (E) after embolization shows CX3CR1-positive intravascular macrophages (green) engulfing fibrin emboli (red). (**F**) Most remaining fibrin emboli (red) at day 11 are not surrounded by macrophages (green), as seen in this confocal image.

occluding emboli varied markedly in the brain and the lungs. In the brain, only 8% of the emboli were surrounded by intravascular monocytes/macrophages by day 3 (Fig. 7, A and B). In contrast, in pulmonary vessels, nearly 95% of the emboli were surrounded by intravascular macrophages as early as 1 day after embolization (Fig. 7C), and these macrophages appeared to be engulfing them over the subsequent 6 days (Fig. 7, D and E). However, beyond 6 days, there was a marked decline in the number of macrophages surrounding the remaining pulmonary intravascular emboli (Fig. 7, C and F). This reduction in macrophages coincided temporally with the acceleration in the rate of angiophagy (Fig. 6E). Because of this inverse relationship, we hypothesize that intravascular macrophages engulf and attempt to degrade the occluding emboli within the vessel but, in the process, may inhibit the endothelial plasticity associated with angiophagy.

### Microvascular recanalization is observed in the mouse and human retina

Vessels in the retina are frequent sites of occlusions owing to spontaneous emboli dislodgment from atherosclerotic and calcific plaques in arteries and heart valves (*20*), or as a result of iatrogenic dislodgment during cardiovascular invasive procedures (*21*). Retinal emboli can cause ischemia and impair tissue functioning, frequently resulting in loss of vision (*5*). We investigated mechanisms of recanalization in mouse retinal vessels by introducing fluorescent emboli through the internal carotid artery and performing high-resolution confocal microscopy of retinal explants. Microvessels in the mouse retina underwent an identical cellular process of endothelial engulfment and embolus extravasation as observed in other organs (fig. S5).

We further explored the possibility of angiophagy in human retinal vessels. We searched for incidences of microvascular occlusions via a retrospective review of fundus photographs with fluorescein angiographies from patients with retinal artery occlusions from the Yale Eye Center from 2002 to 2013. From the 193 cases selected for the study, 9 patients with serial images with evidence of retinal arterial emboli were identified. Careful examination of images collected at multiple time points in each of these nine cases revealed two patients with microvascular emboli that were visible at consecutive time points. In both cases, subsequent imaging 3, 32, or 52 weeks after the first series of imaging (conducted 1 day after symptom onset) demonstrated emboli in the perivascular space adjacent to previously occluded microvessels (Fig. 8, A to E). These microvessels were recanalized, as demonstrated by fluorescein angiograms (Fig. 8, B to E). In patient 2, we observed the apparent resolution of an adjacent area of ischemia, evidenced by the disappearance of a patch of retinal discoloration (Fig. 8, D and E). The occluding embolus had migrated distally from its initial position before it was extravasated (Fig. 8, D and E). Therefore, embolus migration as well as its subsequent extravasation could have contributed to the resolution of tissue ischemia.

## DISCUSSION

Here, we characterized angiophagy in multiple organs using in vivo imaging and histology, as well as human retinal photography. Our study revealed several findings with potential clinical and therapeutic relevance. First, we noted that, after microvascular embolization in mice, there is rapid remodeling of the endothelium adjacent to the occlusion, with lamellipodia projecting toward the embolus and engulfing it within hours. This engulfment appears to be responsible for the mechanical retention of emboli within the vasculature against residual hemodynamic forces beyond 3 to 6 hours after occlusion. Engulfment

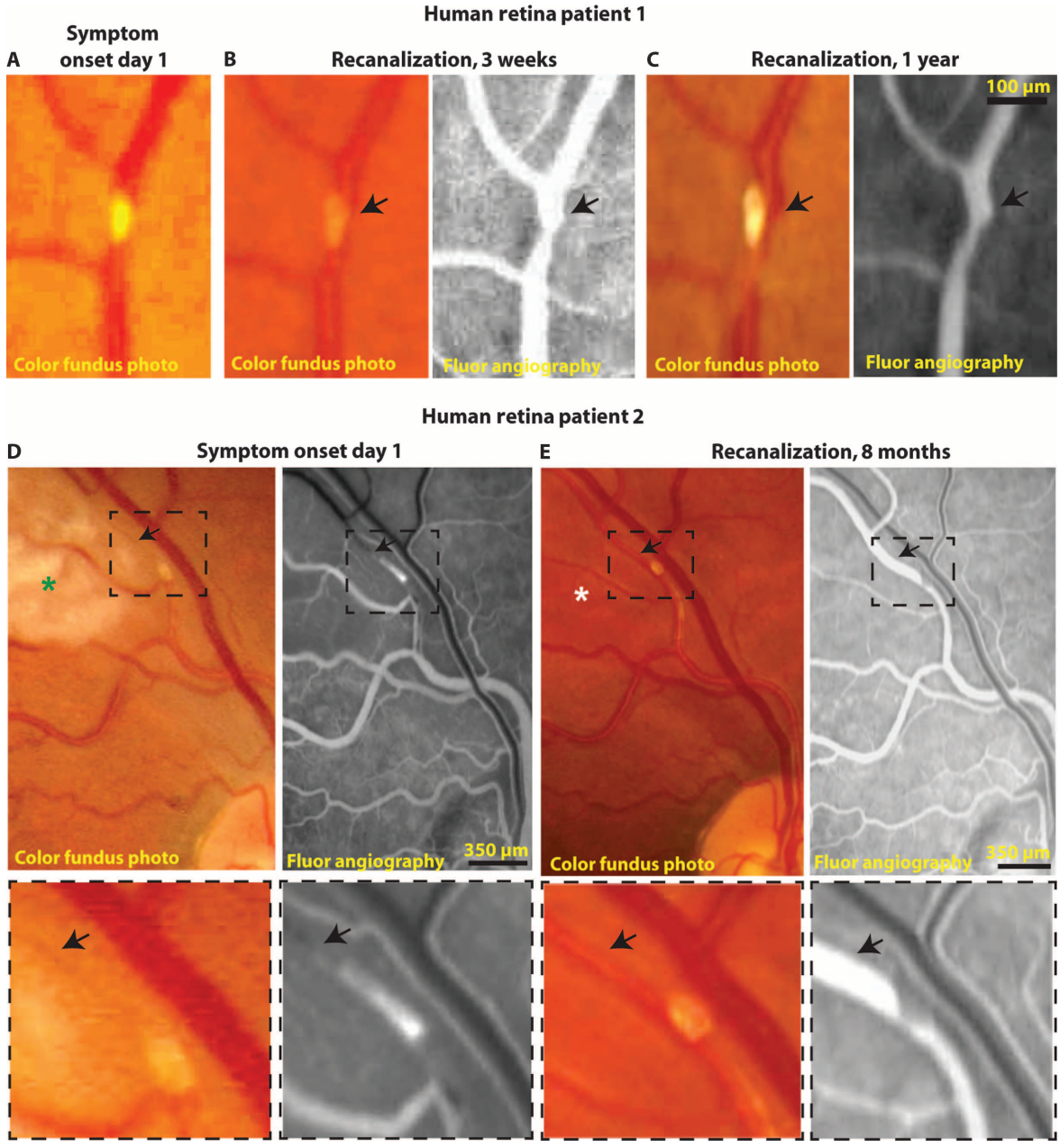


**Fig. 8. Recanalization of retinal microvasculature in humans.** (**A**) Color fundus photograph of patient 1, taken at the time of symptom onset, shows a cholesterol crystal (in yellow) that appeared to be occluding a retinal arteriole (no angiography was available to confirm total occlusion). (**B**) Color fundus photograph and fluorescein angiography of patient 1, taken 3 weeks after symptom onset, show the cholesterol clot and the potential recanalization of the retinal arteriole (black arrow). (**C**) Color fundus photograph and fluorescein angiography of patient 1, taken 1 year after initial symptom onset, show the patent retinal arteriole (black arrow) with the cholesterol embolus persisting in the adjacent perivascular space. (**D**) Color fundus photograph from patient 2, at day 1 after symptom onset, reveals a 70- to 90-μm retinal microvessel (black arrow) in which downstream blood flow was blocked by a cholesterol embolus, likely resulting in retinal ischemia (green asterisk). Fluorescein angiography shows the occluded microvessel (black arrow) with an unperfused segment downstream to the site of occlusion. (**E**) Eight months after initial imaging of the retinal arteriole occlusion in (D), repeat color fundus photography shows that the embolus had moved downstream (blue arrow), but also had been translocated into the perivascular space, as seen clearly in the magnified images (below). The previously occluded vessel was recanalized and patent (black arrow), and the previously observed ischemia in the adjacent tissue was resolved (white asterisk).

may also insulate the emboli from plasma tPA, further reducing the efficiency of fibrinolysis and embolus washout. The 3- to 6-hour window of successful embolus washout in mice is similar to the time window for a favorable clinical response to tPA administration in patients with stroke and myocardial infarction (*22*, *23*). This raises the intriguing possibility that clinical thrombolysis failure beyond 6 hours and the

no-reflow phenomenon—wherein blood flow to ischemic tissues remains impeded despite resolution of the vascular occlusion (*2*)—may be partly mediated by downstream microvascular occlusions that fail to recanalize owing to endothelial clot engulfment.

After the initial envelopment by lamellipodia, emboli were progressively translocated into the perivascular space, leading to blood flow reestablishment and long-term vessel sparing. Although recanalization by angiophagy is limited to relatively small vessels (<80 μm), these constitute the majority of vessels in most organs, including the heart, brain, and lungs. Furthermore, although the time course of angiophagy is on the order of days, it likely plays an important role in maintaining vessel patency and limiting ischemia, given that cell death continues to occur over weeks after microvascular occlusions, especially in the ischemic penumbral regions (*24*).

Another important finding in our study is that angiophagy is a ubiquitous mechanism present in all organs we tested: brain, retina, heart, lungs, and kidneys. In the brain, extravasated fibrin clots were initially engulfed by adjacent pericytes, where they underwent partial degradation, and were later transported across the vessel wall into the parenchyma, where they were phagocytosed and degraded by microglia. In the lungs and kidneys, extravasated emboli were translocated across the adjacent epithelia into the alveolar space and renal tubules, from where they were eliminated. Thus, angiophagy may constitute a previously unknown mechanism for permanent removal of circulating debris from the body via lung alveolar macrophages and the mucociliary stream (*25*), as well as the urinary system.

In the lungs, we found angiophagy to have several unique features. Emboli extravasation was delayed by several days compared to other organs, but eventually accelerated 6 days after embolization, leading to extravasation of most emboli (80%). Although the precise reasons for this delay are unknown, one potential explanation relates to the specialized functions of the microvascular branches of the pulmonary artery. Instead of carrying oxygen to a particular tissue territory, these branches carry deoxygenated blood near the alveolar surface for gas exchange. Although occlusions in these vessels can cause morbidity, they do not cause substantial focal tissue hypoxia. Given that hypoxia induces hypoxia-inducible factor 1α and vascular endothelial growth factor signaling pathways that are critical for endothelial remodeling (*26*), the lack of endothelial hypoxia in lung microvascular embolizations may explain the delay in emboli extravasation. In addition, in stark contrast to microemboli in other organs, we found emboli in the lungs to be quickly engulfed by macrophages within the vasculature. These cells may be attempting to degrade emboli within the vessel lumens but, in that process, may inhibit the endothelial engulfment process. These intriguing findings raise the possibility that immunomodulatory drugs that affect macrophage function, such as corticosteroids, nonsteroidal anti-inflammatories, peroxisome proliferator–activated receptor γ agonists, and others, could have an effect on the rates of emboli retention and extravasation in the lung. Preclinical studies could directly test the effects of such therapeutics.

We explored the possibility of angiophagy in human retinal vessels to determine whether this process is evolutionarily conserved and, toward translation, whether this process might be a therapeutic target. Given its accessibility for imaging and the frequent occurrence of symptomatic embolic occlusions in its microvessels, the retina would be one of the few places where detection of angiophagy in vivo might be possible. Retina photography and angiography of human patients revealed that emboli can be extruded out of occluded microvessels. Given their reflective nature, we predict that these emboli are cholesterol crystals because neither fibrin nor blood clots are reflective and thus are unlikely to be visualized by retina photography. In support of our hypothesis, cholesterol crystals from the aorta and the carotid arteries are widely recognized as the most common cause of retina embolization.

Our experimental mouse data demonstrate unambiguously that various organs undergo a phenomenon of microvascular plasticity and embolus extravasation as seen in the brain. However, one caveat of our study is that in most organs, we were unable to obtain time-lapse in vivo images and thus cannot demonstrate definitively the recanalization and flow restoration of individual vessels as a result of the extravasation process, like in the brain. We also acknowledge that the human retinal images have limitations in spatial and temporal resolution, raising the question of whether an extravasated embolus has completely crossed the microvascular wall, and whether the time course is similar to that in mice. Furthermore, retina photography likely underestimates the frequency of extravasation of emboli, such as those composed of fibrin, because only highly reflective and nondegradable materials like cholesterol crystals can persist over time to be visualized and identified in the adjacent perivascular space. Although these images cannot unambiguously prove that angiophagy occurs in humans, they do provide preliminary evidence suggesting that this microvascular mechanism may be conserved and could thus have potential clinical and therapeutic relevance. Future studies of retinal embolism using optical coherence tomography, adaptive optics, and confocal ophthalmoscopy may provide additional information about the time course and mechanisms of microvascular recanalization in humans. Finally, although we show that emboli can cross into the alveolar and renal tubular spaces, allowing us to speculate that these may be potential routes for permanent removal of circulating debris, we did not directly address the pathophysiological importance of such mechanisms, which remains to be determined in future studies.

Towards translation of our findings into the clinic, we believe that the earlier stages of angiophagy are likely to require therapies aimed at inhibiting the formation of the endothelial envelope around clots to increase washout after microembolisms. For example, drugs that target the actin cytoskeleton or microtubules could be tested for their potential to disrupt the growth of endothelial lamellipodia before they engulf emboli. Such approach could improve the access of adjuvant fibrinolytic agents to emboli lodged in microvessels after stroke or myocardial infarction, leading to reductions in the no-reflow phenomenon (*2*). Once the time window for early washout has passed and emboli are completely engulfed, it is likely that another cellular therapeutic target will be required to enhance the opening of the endothelial barrier and promote emboli extrusion. Although we do not fully understand the mechanisms through which emboli cross the endothelial barrier, matrix metalloproteinase 2/9 (MMP2/9) inhibitors have previously been shown to inhibit angiophagy (*14*, *15*). Therefore, one potential approach to increase embolus extrusion could be to promote MMP2/9 activity at the site of microvascular occlusion.

Further improvement in our understanding of the cellular mechanisms underlying angiophagy may lead to the design of therapies that treat thromboemboli in a variety of organs, as well as iatrogenic microembolic complications from cardiovascular interventions. Inhibition of extravasation through angiophagy could also be relevant in improving intravascular retention of microspheres commonly used for therapeutic embolization procedures in a variety of medical conditions (*27*).

## MATERIALS AND METHODS

### Study design

The aim of our study was to characterize the early features and the precise time course of angiophagy, as well as to explore the potential occurrence of this embolus clearing mechanism in microvessels outside the brain and in humans. We studied embolus washout, early envelope formation, and angiophagy by two-photon live imaging of the cerebral microvasculature in *Tie2-GFP* mice. Angiophagy in the heart and retina was analyzed using cardiac and retinal fixed tissue from *Tie2-GFP* mice. Immunohistochemistry for tPA and electron microscopy were performed on brain tissue from wild-type mice. Studies on angiophagy in the lung and kidney were performed on tissue from wild-type mice. The roles of monocytes and intravascular macrophages in angiophagy were investigated in *CX3CR1-GFP* mice. Sample sizes were decided on the basis of our previous studies (*14*) and ranged from 3 to 52 mice, with up to 309 occlusive events imaged per experiment. Specific parameters for each experiment are provided in the text. Quantifications of retained emboli, tPA levels, and extravasation rates were analyzed with high-resolution confocal microscopy. Quantifications of early emboli engulfment were performed with two-photon live imaging. The transmission electron micrographs in Fig. 2 were obtained from the collection at the open connectome project (http://www.openconnectomeproject.org) with permission (D. Bock and C. Reid) (*28*). Color fundus photographs and fluorescence angiographs from human patients with retinal emboli were collected at Yale Eye Center.

### Experimental animals

*Tg(TIE2GFP)*287Sato/J (stock number 003658), *FVB-Tg*(Cspg4-cre) 1AKik (Jackson Laboratory #008533), B6.129*(Cg)-Gt(ROSA) 26Sor*$^{tm4(ACTB-tdTomato,-EGFP)Luo}$/J (Jackson Laboratory #007676), B6.129P-*CX3CR1tm1*Litt/J (Jackson Laboratory #005582), and CD1 mice (Charles River) ages 4 to 8 weeks were used for all experiments. All experiments were in compliance with guidelines from the Yale and Northwestern University Institutional Animal Care and Use Committee.

### Embolization procedures

Fluorescent emboli were generated as described in Supplementary Methods. Mice were anesthetized with an intraperitoneal injection of ketamine/xylazine (100 mg of ketamine/10 mg of xylazine per kilogram of body weight). A midline ventral incision in the neck was made, and the common, external, and internal carotid arteries were freed from the connective tissue and ligated with sutures. A small incision was made in the common carotid artery, and a custom-made catheter, preloaded with the fluorescently labeled emboli suspension, was inserted into common carotid artery. The cholesterol or fibrin emboli solution (150 μl, ~80 embolic particles per microliter) was injected gradually over a period of 1 to 2 min. For embolization of cerebral and retinal circulations, the catheter was advanced from the common carotid into the internal carotid artery, followed by injection of the emboli suspension. For embolization of the coronary and renal circulations, the catheter was inserted into the common carotid artery and advanced in a retrograde manner to enter the heart, followed by the injection of the emboli suspension into the left ventricle. After the injection of the emboli suspension, the catheter was removed and the common carotid was sealed with cyanoacrylate glue. Sutures ligating the common, internal, and external carotid arteries were removed, and normal blood flow was restored. The lungs were embolized by tail vein injections. tPA (Activase, 1 mg/kg, Genentech) was administered intravenously 3 and 6 hours after embolization.

### Human retina photography and angiography

Yale University Human Investigation Committee approved the study. We retrospectively reviewed all fundus photographs and fluorescein angiographies from patients with retinal artery occlusion ($n$ = 193) from Yale Eye Center from 2002 to 2013. Nine of these patients who had retinal arterial emboli were selected for this study. Human retina photography and fluorescein angiography were performed with Topcon fundus camera. For fundus photography, 35° and 50° photos were taken. For fluorescein angiography, fluorescein sodium was injected intravenously followed by imaging of fundus starting at 5 s after injection of fluorescein and continued for 10 min.

### Statistical analyses

Statistical analyses were performed with GraphPad version 6. Comparisons between two time points were conducted with the unpaired $t$ test. Comparisons of more than two time points were conducted with one-way ANOVA with Tukey's multiple comparison test. Verification of statistical analysis was performed with repeated-measures ANOVA with significance level α of 0.05 (95% confidence intervals). All data are means ± SEM. $P < 0.05$ was considered to be significant.

## SUPPLEMENTARY MATERIALS

www.sciencetranslationalmedicine.org/cgi/content/full/6/226/226ra31/DC1

Methods

Fig. S1. Fibrin emboli in the brain are degraded over time.

Fig. S2. Fibrin emboli are degraded in pulmonary alveoli.

Fig. S3. A large microsphere extravasated out from a pulmonary vessel.

Fig. S4. Extravasation of a microsphere from the renal pelvis microvasculature.

Fig. S5. Recanalization of retinal microvasculature in mice.

Movie S1. Endothelial cellular envelop surrounding a fibrin clot in a brain microvessel.

Movie S2. Endothelial cellular envelop surrounding a fibrin clot in a coronary microvessel.

Movie S3. Long endothelial filopodia are present at baseline in unoccluded microvessels.

Movie S4. Short endothelial filopodia are present at baseline in unoccluded microvessels.

Movie S5. Fibrin embolus extravasated out from a large pulmonary microvessel.

## REFERENCES AND NOTES


1. L. R. Caplan, M. Hennerici, Impaired clearance of emboli (washout) is an important link between hypoperfusion, embolism, and ischemic stroke. *Arch. Neurol.* **55**, 1475–1482 (1998).
2. S. H. Rezkalla, R. A. Kloner, No-reflow phenomenon. *Circulation* **105**, 656–662 (2002).
3. R. A. Kloner, R. E. Rude, N. Carlson, P. R. Maroko, L. W. DeBoer, E. Braunwald, Ultrastructural evidence of microvascular damage and myocardial cell injury after coronary artery occlusion: Which comes first? *Circulation* **62**, 945–952 (1980).
4. N. Galiè, N. H. S. Kim, Pulmonary microvascular disease in chronic thromboembolic pulmonary hypertension. *Proc. Am. Thorac. Soc.* **3**, 571–576 (2006).
5. D. J. McBrien, R. D. Bradley, N. Ashton, The nature of retinal emboli in stenosis of the internal carotid artery. *Lancet* **281**, 697–699 (1963).
6. E. J. Topol, J. S. Yadav, Recognition of the importance of embolization in atherosclerotic vascular disease. *Circulation* **101**, 570–580 (2000).
7. D. M. Moody, M. A. Bell, V. R. Challa, W. E. Johnston, D. S. Prough, Brain microemboli during cardiac surgery or aortography. *Ann. Neurol.* **28**, 477–486 (1990).
8. J. H. Rapp, X. M. Pan, F. R. Sharp, D. M. Shah, G. A. Wille, P. M. Velez, A. Troyer, R. T. Higashida, D. Saloner, Atheroemboli to the brain: Size threshold for causing acute neuronal cell death. *J. Vasc. Surg.* **32**, 68–76 (2000).
9. S. E. Vermeer, N. D. Prins, T. den Heijer, A. Hofman, P. J. Koudstaal, M. M. B. Breteler, Silent brain infarcts and the risk of dementia and cognitive decline. *N. Engl. J. Med.* **348**, 1215–1222 (2003).

10. D. Russell, Cerebral microemboli and cognitive impairment. *J. Neurol. Sci.* **203–204**, 211–214 (2002).
11. R. S. Saber, W. D. Edwards, K. R. Bailey, T. W. McGovern, R. S. Schwartz, D. R. Holmes, Coronary embolization after balloon angioplasty or thrombolytic therapy: An autopsy study of 32 cases. *J. Am. Coll. Cardiol.* **22**, 1283–1288 (1993).
12. J. I. Iliopoulos, M. J. Zdon, B. G. Crawford, G. E. Pierce, J. H. Thomas, A. S. Hermreck, Renal microembolization syndrome. A cause for renal dysfunction after abdominal aortic reconstruction. *Am. J. Surg.* **146**, 779–783 (1983).
13. B. V. Zlokovic, L. Wang, N. Sun, S. Haffke, S. Verrall, N. W. Seeds, M. J. Fisher, S. S. Schreiber, Expression of tissue plasminogen activator in cerebral capillaries: Possible fibrinolytic function of the blood-brain barrier. *Neurosurgery* **37**, 955–961 (1995).
14. C. K. Lam, T. Yoo, B. Hiner, Z. Liu, J. Grutzendler, Embolus extravasation is an alternative mechanism for cerebral microvascular recanalization. *Nature* **465**, 478–482 (2010).
15. J. Grutzendler, Angiophagy: Mechanism of microvascular recanalization independent of the fibrinolytic system. *Stroke* **44**, S84–S86 (2013).
16. R. Harb, C. Whiteus, C. Freitas, J. Grutzendler, In vivo imaging of cerebral microvascular plasticity from birth to death. *J. Cereb. Blood Flow Metab.* **33**, 146–156 (2013).
17. G. Heusch, R. Schulz, M. Haude, R. Erbel, Coronary microembolization. *J. Mol. Cell. Cardiol.* **37**, 23–31 (2004).
18. J. Herrmann, Peri-procedural myocardial injury: 2005 update. *Eur. Heart J.* **26**, 2493–2519 (2005).
19. W. M. Thurlbeck, B. Castleman, Atheromatous emboli to the kidneys after aortic surgery. *N. Engl. J. Med.* **257**, 442–447 (1957).
20. C. D. Reimers, R. J. Williams, M. Berger, H. J. Wisnicki, R. F. Tranbaugh, Retinal artery embolization: A rare presentation of calcific aortic stenosis. *Clin. Cardiol.* **19**, 253–254 (1996).
21. J. A. Vos, M. H. van Werkum, J. H. Bistervels, R. G. Ackerstaff, S. C. Tromp, J. C. van den Berg, Retinal embolization during carotid angioplasty and stenting: Periprocedural data and follow-up. *Cardiovasc. Intervent. Radiol.* **33**, 714–719 (2010).
22. W. Hacke, M. Kaste, E. Bluhmki, M. Brozman, A. Dávalos, D. Guidetti, V. Larrue, K. R. Lees, Z. Medeghri, T. Machnig, D. Schneider, R. von Kummer, N. Wahlgren, D. Toni; ECASS Investigators, Thrombolysis with alteplase 3 to 4.5 hours after acute ischemic stroke. *N. Engl. J. Med.* **359**, 1317–1329 (2008).
23. W. J. Rogers, L. J. Bowlby, N. C. Chandra, W. J. French, J. M. Gore, C. T. Lambrew, R. M. Rubison, A. J. Tiefenbrunn, W. D. Weaver, Treatment of myocardial infarction in the United States (1990 to 1993). Observations from the National Registry of Myocardial Infarction. *Circulation* **90**, 2103–2114 (1994).
24. M. Wang, J. J. Iliff, Y. Liao, M. J. Chen, M. S. Shinseki, A. Venkataraman, J. Cheung, W. Wang, M. Nedergaard, Cognitive deficits and delayed neuronal loss in a mouse model of multiple microinfarcts. *J. Neurosci.* **32**, 17948–17960 (2012).
25. W. G. Hocking, D. W. Golde, The pulmonary-alveolar macrophage. *N. Engl. J. Med.* **301**, 580–587 (2010).
26. N. V. Iyer, L. E. Kotch, F. Agani, S. W. Leung, E. Laughner, R. H. Wenger, M. Gassmann, J. D. Gearhart, A. M. Lawler, A. Y. Yu, G. L. Semenza, Cellular and developmental control of $O_2$ homeostasis by hypoxia-inducible factor 1$\alpha$. *Genes Dev.* **12**, 149–162 (1998).
27. C. P. Derdeyn, V. B. Graves, M. S. Salamat, A. Rappe, Collagen-coated acrylic microspheres for embolotherapy: In vivo and in vitro characteristics. *AJNR Am. J. Neuroradiol.* **18**, 647–653 (1997).
28. D. D. Bock, W. C. A. Lee, A. M. Kerlin, M. L. Andermann, G. Hood, A. W. Wetzel, S. Yurgenson, E. R. Soucy, H. S. Kim, R. C. Reid, Network anatomy and in vivo physiology of visual cortical neurons. *Nature* **471**, 177–182 (2011).

**Funding:** This project was supported by grants R01HL106815 and R01AG027855 (J.G.) and fellowship T32HL007950 (S.G.). **Author contributions:** Project conception and overall supervision (J.G.), experimental design and execution (S.M., B.H., L.J., C.K.L., T.Y., S.G., P.Y., G.R., and J.G.), data analysis (J.G., S.M., B.H., and L.J.), design and analysis of human retina data (R.A.A. and B.P.H.), and manuscript writing (J.G., with input from S.M. and S.G.). **Competing interests**: Three of the authors (J.G., C.K.L., and T.Y.) are inventors on a U.S. patent application filing (10 March 2011) based on this work [publication number: U.S. 20110223128 A1; application number: 13/045265]. **Data and materials availability:** Transmission electron micrographs were obtained from the open connectome project with permission (D. Bock, W. Lee, and R. Reid). Genentech provided recombinant tPA under a materials transfer agreement.

Submitted 15 May 2013
Accepted 2 January 2014
Published 5 March 2014
10.1126/scitranslmed.3006585

**Citation:** J. Grutzendler, S. Murikinati, B. Hiner, L. Ji, C. K. Lam, T. Yoo, S. Gupta, B. P. Hafler, R. A. Adelman, P. Yuan, G. Rodriguez, Angiophagy prevents early embolus washout but recanalizes microvessels through embolus extravasation. *Sci. Transl. Med.* **6**, 226ra31 (2014).

Science Translational Medicine
AAAS

# Angiophagy Prevents Early Embolus Washout But Recanalizes Microvessels Through Embolus Extravasation

Jaime Grutzendler *et al.*

*Sci Transl Med* **6**, 226ra31 (2014);
DOI: 10.1126/scitranslmed.3006585

Editor's Summary

## Beyond the Brain: Angiophagy Clears Clots in Other Organs, Too

Vessels in the body can be obstructed by tiny emboli, which are usually blood clots, but can also be cholesterol crystals or fragments of atherosclerotic plaques. Much like a bathroom drain, these clogged "pipes" can be cleared mechanically (hemodynamic forces) or biochemically (fibrinolysis). Now, Grutzendler and colleagues describe another possible clearance mechanism called angiophagy, where endothelial cells, which line the blood vessels, can actively remove clots from the vasculature.

Mice were given fibrin or cholesterol clots by a syringe to mimic the embolization process (where clots build up in the vasculature). Using sophisticated live-imaging techniques, Grutzendler *et al.* then peered into the blood vessels of mice to watch clot dynamics. They saw that endothelial cells were able to engulf these emboli in the microvasculature of the heart and the brain, causing them to exit the blood vessel entirely and allowing flow to resume in the vessel. The authors called this process "angiophagy" and noted that it occurred as early as 1 day after clot formation, with most clots being removed by day 4. Angiophagy also appeared to play a role in clot clearance from the mouse kidney, eye, and lung microvasculature, suggesting that this is a general means of extravasation and recanalization. Looking retrospectively at images of human retinal vessels, Grutzendler *et al.* were able to see microvascular emboli in the perivascular spaces, just outside the blood vessels, suggesting migration of the clot across the vessel wall.

Live imaging over time in several organ systems has shed light on the dynamics of this clot-clearing process. One limitation of angiophagy is that endothelial lamellipodia—while trying to engulf the clot for removal—apparently limit access of exogenous clot-busting drugs and endogenous fibrin-degrading enzymes to the emboli, thus reducing the early effectiveness of washout by other mechanisms. Nevertheless, knowing the time course of angiophagy in vivo in mice could help develop new anti-embolic drugs that could prevent widespread complications from medical procedures, aging, and disease.



*Science Translational Medicine* (print ISSN 1946-6234; online ISSN 1946-6242) is published weekly, except the last week in December, by the American Association for the Advancement of Science, 1200 New York Avenue NW, Washington, DC 20005. 

*Science Translational Medicine* (print ISSN 1946-6234; online ISSN 1946-6242) is published weekly, except the last week in December, by the American Association for the Advancement of Science, 1200 New York Avenue NW, Washington, DC 20005. 